INVESTIGATING THE USE OF AI-BASED ANALYSES OF FUNDUS IMAGES FOR RETINOPATHY SCREENING AND VASCULAR RISK STRATIFICATION IN PATIENTS WITH DIABETES: AN EXPLORATORY STUDY

Technical Report 2:

Vascular risk stratification

Annibale Cois[1,2], Rifqah Roomaney[1], Eric Falletisch[3]

[1] Burden of Disease Research Unit, South African Medical Research Council

[2] Division of Epidemiology and Biostatistics, School of Public Health, University of Cape Town

[3] Somerset Eye, Somerset West

JUNE 2026

ISBN: 978-1-928340-92-8
Date of Publication: 22/06/2026

SUGGESTED CITATION

Cois A, Roomaney RA, Falletisch E (2026). *Investigating the use of AI-based analyses of fundus images for retinopathy screening and vascular risk stratification in patients with diabetes: an exploratory study. Technical Report 2: Vascular risk stratification*. Cape Town: South African Medical Research Council. ISBN: 978-1-928340-92-8.

ACKNOWLEDGEMENTS

This study would not have been possible without the collaboration of **Dr Elmo Pretorius** (*Internalmed* endocrinologist practice, https://internalmed.co.za/) who allowed the study to be conducted within the practice and provided valuable support to the research team throughout the project, and **Sr Marion Potterton**, who managed professionally and effectively the process of contacting patients, acquiring their informed consent, and extracting the data from the clinical records. We also want to acknowledge **Mr Christofer Fielding**, who collaborated on the data collection and set up the system for the automatic extraction of laboratory data from the patients' folders.

CONTENT

EXECUTIVE SUMMARY

This exploratory study investigated the potential use of AI-based analyses of retinal fundus images for vascular risk stratification among patients with diabetes attending a specialist endocrinology practice in South Africa. The study forms part of the Retinography Project, an initiative aimed at improving the accessibility and efficiency of diabetic retinopathy screening using portable retinal imaging devices and automated AI-supported image analysis.

A total of 200 adult diabetic patients consented to participate. Retinal fundus images were analysed using automated deep learning pipelines to extract quantitative vascular features, including vessel calibre, tortuosity, vessel density, and fractal dimension. These retinal parameters were then examined in relation to systemic biomarkers and clinically documented diabetic complications, including chronic kidney disease, cardiovascular disease, and peripheral neuropathy.

The findings provide preliminary evidence that retinal vascular morphology is associated with several important systemic indicators of diabetic disease severity and vascular dysfunction. Reduced kidney function, reflected by lower estimated glomerular filtration rate (eGFR) and higher serum creatinine levels, was associated with increased venular calibre and tortuosity. Poor glycaemic control, measured through HbA1c, was associated with reduced fractal dimension and vessel density, suggesting loss of vascular complexity and microvascular rarefaction. Measures of venular tortuosity were also associated with adverse lipid profiles.

The study further developed a proof-of-concept deep learning model for the identification of chronic kidney disease directly from retinal fundus images. Although model performance was modest (mean AUC = 0.73), the results demonstrate the feasibility of using retinal imaging as a low-cost, non-invasive adjunct tool for systemic vascular risk stratification in diabetic populations. Attention analyses using Grad-CAM suggested that the model relied on biologically plausible retinal regions and vascular structures during prediction.

The study was exploratory in nature and should primarily be interpreted as a proof-of-concept investigation conducted in a real-world clinical environment. The sample size was relatively small, and the analyses involved multiple comparisons without formal correction procedures. Consequently, the reported associations should not be interpreted as definitive evidence of causality or clinical utility. Instead, they provide important signals and hypotheses for future studies.

Despite these limitations, the findings align with the growing field of oculomics, which conceptualises the retina as a readily accessible biomarker of systemic vascular health. The results support the feasibility of integrating AI-assisted retinal imaging into broader diabetic care pathways, particularly in resource-constrained settings where traditional laboratory-based risk stratification may be difficult to implement at scale.

INTRODUCTION

Diabetes and vascular disorders

Both microvascular and macrovascular disorders –which are different manifestations of the same underlying pathological atherosclerotic mechanism– are common complications of diabetes and primary causes of morbidity and mortality in diabetic patients.[1–3] The frequency of complications[4] and the globally rising number of diabetic people result in an already enormous and rapidly growing societal cost.[5] A variety of studies in different geographical contexts have provided ample evidence that both type 1 and type 2 diabetes cause substantial direct and indirect financial burden on the economy of countries, with a global economic burden estimated at 1.31 trillion USD, or 1.8% of the world gross domestic product in 2015.[6] At the individual level, the onset of complications reduces the quality of life, particularly when microvascular and macrovascular disorders coexist[5,7–9]

Microvascular alterations associated with diabetes result in damage at the level of the retina (Diabetic retinopathy), kidneys (Diabetic nephropathy) and the peripheral nervous system (Diabetic neuropathy). Organ damage can be extensive and cause severe disability and death. Diabetic retinopathy is a leading cause of vision loss globally, and, in many countries, it is the most frequent cause of acquired vision loss in middle-aged people.[10–13] A 2012 systematic review and meta-analysis of population-based studies on prevalence and risk factors for DR estimated that 34.6% of diabetic patients have some degree of DR, and more than 10% are afflicted by vision-threatening forms of the disease (vision-threatening diabetic retinopathy [VTDR], defined as severe non-proliferative DR, proliferative PD [PDR] or the presence of diabetic macular oedema [DME]).[14] Diabetic nephropathy is the most common reason for renal replacement therapy worldwide.[5] It affects approximately 40% of type 1 and type 2 diabetic patients.[15] Diabetic neuropathy is associated with a host of severe outcomes, such as foot amputations (as the most frequent non-traumatic cause of lower limb amputation), chronic pain, muscle weaknesses and atrophy.[16]

Macrovascular disorders of relevance for diabetic patients include ischaemic heart disease, peripheral arterial disease and stroke (cardiovascular diseases, CVDs) which, globally, affect almost a third of patients with type 2 diabetes,[7] and are the primary cause of death in people with either type 1 or type 2 diabetes.[17,18] In the last four decades, since the first suggestions arising from the Framingham study,[19] investigations conducted in diverse populations and contexts have repeatedly confirmed the heightened risk of CVDs among diabetic patients.[17,20,18] Results from a large meta-analysis of 102 prospective studies from the Emerging Risk Factors Collaboration, including data on more than 650 000 individuals

indicate that, overall, diabetes is associated with about a two-fold excess risk for a wide range of cardiovascular diseases, independently from other risk factors.[21]

The time of onset of vascular complications in patients with diabetes has been shown to be a function of age, population group and genetic background, type of treatment and level of glycaemic control, with microvascular complications generally showing an early onset compared to macrovascular complications.[22] Coherently with their hypothesised common pathogenesis (endothelial dysfunction and atherosclerosis), studies have shown significant associations between the different categories of vascular disease, with large commonalities in terms of coexistence, development and response to intervention against metabolic abnormalities.[2,23]

Fundus examination in diabetic patients

Periodic, systematic examination of the interior surface of the eye opposite the lens (*fundus*, which includes the retina, optic disc, macula, fovea, and posterior pole) for detection of microvascular alterations has long since recognised and standardised procedures have been included in major national and international clinical management guidelines for diabetic patients.[24–27] The recommendations are supported by robust evidence that fundus examination can detect early signs of diabetic retinopathy and that various treatments exist (laser treatment, intravitreal injections, and eye surgery among others) which are effective in preventing progression to severe vision-threatening forms of the disease (vision-threatening diabetic retinopathy, severe non-proliferative retinopathy, proliferative retinopathy and the presence of macular oedema).[28,29,12]

Various techniques are used to screen for diabetic retinopathy, with different levels of sensitivity and specificity, requirements in terms of training of health professionals and cost. The most common techniques include direct and indirect ophthalmoscopy, slit-lamp biomicroscopy, mydriatic and nonmydriatic retinal photography, and optical coherence tomography.[30]

In recent years, advances in wide-field non-mydriatic camera technology and artificial intelligence (AI) diagnostic algorithms have opened new possibilities for implementing low-cost screening programs for the early detection of diabetic retinopathy. The interpretation of retinal images obtained with portable cameras which do not require pharmacologic dilation of the pupil and can be operated by non-specialists through AI deep learning algorithms has achieved excellent diagnostic performance in detecting early stages of diabetic retinopathy, with diagnostic accuracy comparable to the grading by retinal specialists.[31] Commercial AI screening systems have recently obtained regulatory approval in many countries. In South

Africa, two screening systems are commercially available and accepted for reimbursement under the chronic illness benefit for diabetes by the leading private health insurer.[32] AI systems offer substantial benefits for health care by (1) reducing the reliance on manual specialist work, (2) ensuring homogeneous and adequate performance (in terms of sensitivity and specificity in identifying early stages of diabetic retinopathy) which compare favourably with manual screening performed by non-specialists, (3) reducing the overall cost. AI systems can be deployed at the primary/secondary level of care, increasing accessibility and reducing reliance on healthcare provider engagement and patient compliance with referrals.[33–35]

Current available, regulatory-approved, AI systems for the analysis of fundus images for clinical and screening use only focus on the detection of high-incidence ocular diseases, such as diabetic retinopathy, age-related macular degeneration, glaucoma, and retinopathy of prematurity.[34,36,37] However, the research on the automatic analysis of fundus images for disease detection (often grouped under the umbrella term of *oculomics*) has recently broadened its scope to encompass applications to more general vascular risk stratification, including cardiovascular risk stratification. This new area of study founds its rationale in the cited strict etiologic and epidemiological relationships between different categories of vascular alterations and the repeated finding that microvascular alterations in the retina are strongly predictive of future cardiovascular events, including coronary heart disease and stroke, the development of neurogenerative conditions, and associated with all-cause mortality.[38–43] Analytical techniques or the automatic extraction of retinal vascular parameters based on machine learning/deep learning (ML/DL) have shown high accuracy in predicting cardiometabolic risk factors and major cardiovascular events in selected populations,[44–50] and created the basis for the development of rapid, reliable, and cost-effective cardiovascular risk stratification tools for high risk (such as diabetic) patients, with potential further applicability as more general screening tools in primary health care. These tools are potentially advantageous alternatives to current risk assessment tools based on a combination of blood test results and/or multiple anthropometric measurements such as the Framingham[51] and the WHO cardiovascular risk scores[52], which have shown limitations in specific ethnic groups and intermediate risk profile patients[53,54].

Despite these encouraging results from studies in highly controlled environments, implementation of AI based risk stratification methods in clinical routine is still in its infancy. It is generally acknowledged that, before routine implementation, more research is needed (1) to develop algorithms with higher accuracy and predictive abilities, (2) to improve the understanding of the predictive mechanisms beyond the ‘black-box approach of most

ML/DL tools, (3) to improve the 'robustness' of the current algorithm when applied to fundus images acquired with different hardware and of varying technical characteristics and quality levels, (4) and to evaluate their performance and limitations in real-world environments.[36,45,50,55]

The retinography project

At the beginning of 2023, the Diabetic Evaluation Clinic (DEC) in the Somerset Eye practice of Dr Eric Falletisch Inc (https://www.somerseteye.co.za/) initiated a project aimed at improving the timeliness and cost-effectiveness of screening for retinopathy among diabetic patients in their catchment area, by modifying the current situation where the DEC acts as the first level of screening for patients referred by their primary care providers or self-referred. While the service has the resources to thoroughly evaluate the diabetic eye, the type of evaluation (an hour-long appointment scheduling, requiring patients to travel to the Clinic) makes it not well suited to mass screening, for reasons of cost and ease of access for patients in different locations.

The *Retinography* project (www.retinography.co.za), aims to implement an integrated screening model, where the DEC (1) supports primary healthcare providers of diabetic patients (physicians, general practitioners) in establishing easily accessible screening facilities for signs of diabetic retinopathy (including providing training to optometrists, general practitioners and other health workers for the correct use of fundus cameras) and (2) provides specialised diagnostic and therapeutic support for those at risk according to the preliminary screening.

Figure 1: The Retinography project logo

For diabetic care facilities with high numbers of patients (such as specialist endocrinology practices), fundus cameras are directly deployed to the facility, while in case of relatively low diabetic patient load (such as for general practitioners), the facility is associated with a nearby optometrist with the availability of adequate hardware. In both cases, standardised

retinal photos taken with the cameras within the practice (or nearby optometrist) are screened in real-time by an AI system and only patients failing the screening are referred to the DEC, which is more appropriately functioning at the secondary level, with only those who fail both primary and secondary screening being referred onto ophthalmology (tertiary level) for treatment. With this approach, screening is more efficiently delegated at the primary eye care level with the AI system standardising the quality of the assessment, and a network of cameras distributed throughout the territory, together with the lower cost of the screening, improving accessibility.

The first phase of the project started in March 2023 with the deployment of a fundus camera (iCare Centervue DRS Plus, https://www.icare-world.com/product/icare-drsplus/) at a specialist endocrinologist practice (https://internalmed.co.za/). Since then, the standard assessment procedure for all new adult diabetic patients attending medical consultation at the practice (and for all old patients who did not have an eye screening in the previous 12 months) includes an AI-based screening administered by the practice nurse, who has undergone training on the use of the fundus camera. The automatic report generated in real-time by the AI system is used for referral to specialist ophthalmologic evaluation and treatment for those failing the screening test.

The flowchart in Figure 2 illustrates the various phases of the process.

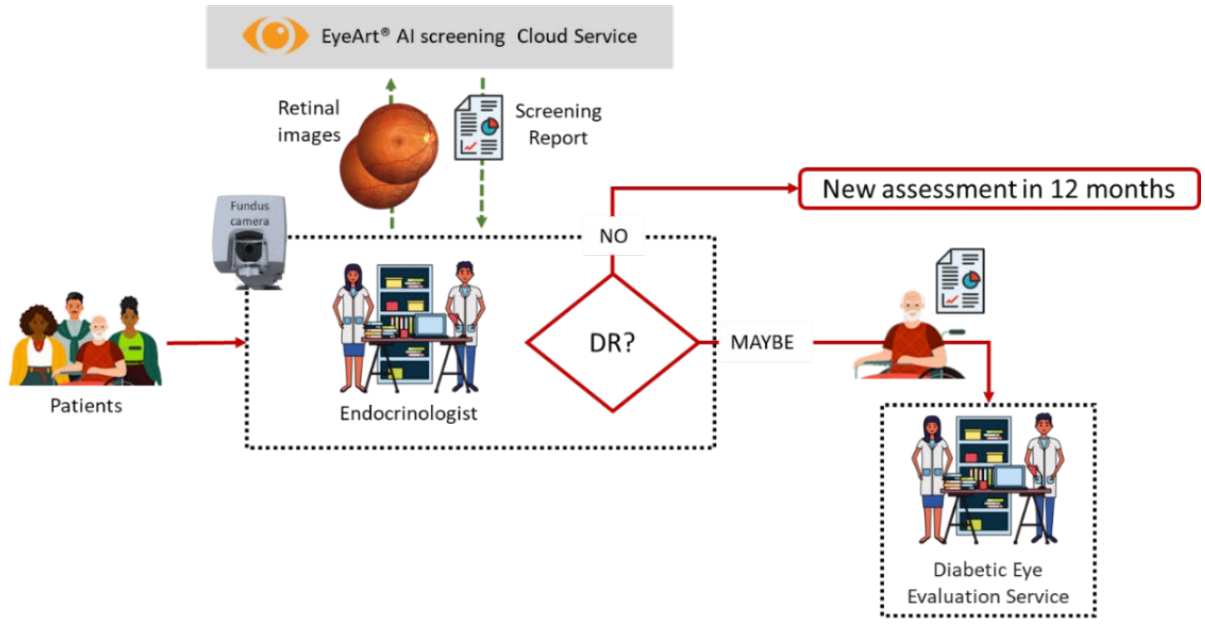

Figure 2: Summary representation of the screening process

The retinal photographs taken during the assessment are saved in the electronic individual patient folders, together with the assessment report, blood test results and medical history, thus offering the possibility of further analyses.

This study aimed at using the available information to 1) investigate the relationships between retinal parameters, presence/absence of comorbidities/complications and laboratory biomarkers and 2) develop a proof-of-concept predictive model for systemic diabetes complications, quantify its performance and gain insights on its decision mechanisms.

METHODS

Population and sample

The target population for this study consists of all adult patients (18 years and over) of the endocrinologist practice with a diagnosis of Diabetes Mellitus (ICD-10 diagnostic codes E10-E11) who underwent AI-based screening for diabetic retinopathy between March 2023 and February 2025.

The sampling took a census approach, and all eligible patients were contacted for participation and enrolled in the study if they consented. Formal eligibility and exclusion criteria were:

Eligibility criteria:

- 18 years and older
- Diagnosis of diabetes mellitus
- Underwent AI-based screening during the study period
- Able and willing to provide informed consent

Exclusion criteria:

- Minor
- Already in the care of an ophthalmologist
- AI-screening carried out outside the study period
- Unwilling or unable (for severe mental illness or disability) to provide informed consent.

Eligible patients were contacted by email by the practice nurse. The email contained (1) a plain language description of the study, its objectives, potential benefits and risks, (2) clarification that participation/non participation in the study had no effect regarding the clinical services received in the practice, (3) the contact numbers/email of the PI for further

information, and (4) the request of consent for extraction of anonymised demographic and clinical data from their electronic folder, including retinal photographs and the AI report. A reply to the email including a signed, scanned copy of the declaration of consent was regarded as a valid expression of consent. Alternatively, the patients were able to express their consent by filling out an online form. No response was followed by a reminder after 2 weeks, and further lack of reply was considered a refusal.

Data extraction

The practice nurse extracted demographic (age, gender) and clinical characteristics (date of diabetes diagnosis, type of diabetes, general medical history and presence of other chronic diseases) of the consenting patients from their paper folders and entered the data in an electronic spreadsheet. The spreadsheet did not include any direct identifier of the participants, who were assigned a unique identification code for the purpose of the study.

A locally deployed large language model was used to extract information included in PDF format in the electronic patient folders, namely the results of the AI screening and the laboratory results (blood and urine tests). When multiple series of laboratory results were available, the tests carried out on the date closest to the date of the AI report were considered. The extracted data were manually checked for inconsistencies and corrected when necessary. The extracted results were linked to the demographic and clinical data by means of the study identification code.

The original, high-resolution, retinal images associated with the AI report were extracted and linked to the demographic and clinical data by means of the study identification code. Four images (2 per eye, centred in the optic disc in the macula as per common practice) were available for each patient.

All extraction and anonymisation procedures were carried out in the practice, and only the anonymised datasets (demographic and clinical information, AI screening results, laboratory results and retinal images) were uploaded to protected cloud storage and made available to the investigators for the analyses. The documents linking anonymised unique identifiers with personal information, allowing for the identification of patients (necessary in case of findings requiring referral), were kept at the practice, with the exclusive availability to the PI and clinical supervisor of the study.

Data analysis

Descriptives

Sociodemographic and clinical characteristics of participants were described as median and interquartile range (IQR) for continuous variables and percentages for categorical variables, separately for males and females.

Relationships between vascular parameters, comorbidities and biomarkers

Extraction of vascular features

We used a validated deep learning pipeline (AutoMorph[56]) for automated segmentation and analysis of retinal vascular morphology on fundus photographs to extract a comprehensive panel of quantitative vascular parameters with clinically-relevant interpretation, as summarised in Figure 3.

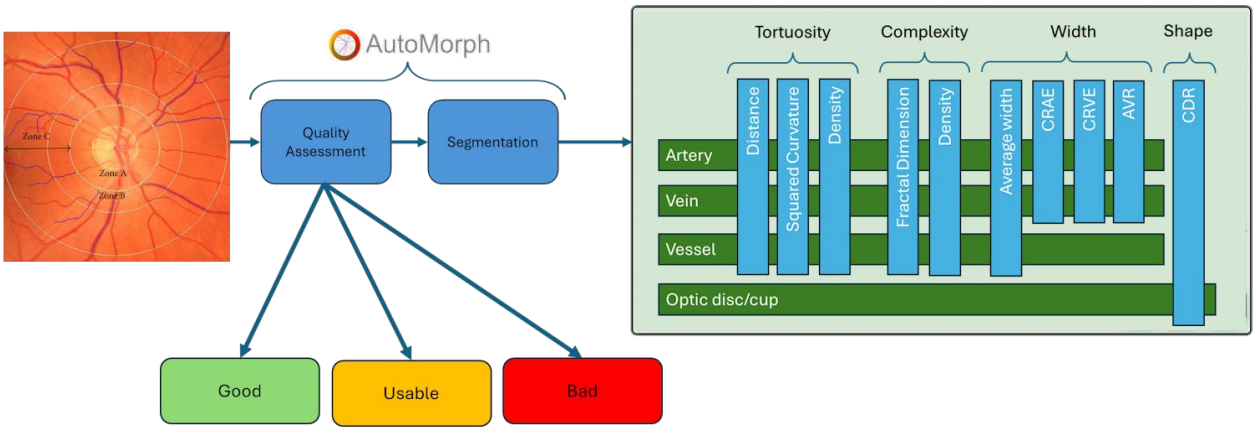

Figure 3: Extraction of vascular parameters

Parameters were extracted for the overall vasculature as well as separately for the arterial and venous networks. The parameter set included measures of:

1. Vascular network **complexity**: *fractal dimension* (FA);
2. Vascular network **sparseness**: *vessel density (VD)*;
3. Vascular **calibre**: average vessel width (AVW), central retinal artery equivalent (CRAE) and central retinal vein equivalent (CRVE), the latter two calculated with both the Hubbard and Knudtson formulae;
4. vascular **tortuosity**: *distance tortuosity*, *squared curvature tortuosity*, and *tortuosity density*.

The *cup-to-disc ratio* (*CDR*) was also included, measured in both the vertical and horizontal planes.[56,57]

Parameters were extracted across two retinal regions of interest (ROIs): Zone B (the peripapillary ring, one to two disc diameters from the optic disc margin) and Zone C (the mid-peripheral zone, two to three disc diameters from the disc margin), in addition to a global measurement without zone stratification. (Figure 4)

Figure 4: Regions of interest for the calculation of vascular parameters

In total, 62 retinal vessel parameters were included in the analysis (Table 1).

Table 1: Retinal parameters

		Zone			Vessel type		
Class	**Parameter**	**B**	**C**	**All**	**Arteries**	**Veins**	**All**
Tortuosity measures	Distance tortuosity	x	x	x	x	x	x
	Tortuosity density	x	x	x	x	x	x
	Squared curvature tortuosity	x	x	x	x	x	x
Complexity measures	Fractal dimension	x	x	x	x	x	x
Sparseness measures	Vessel density	x	x	x	x	x	x
Calibre measures	Average vessel width	x	x	x	x	x	x
	CRAE Hubbard	x	x		x		
	CRAE Knudtson	x	x		x		
	CRVE Hubbard	x	x			x	
	CRVE Knudtson	x	x			x	

The analysis pipeline included a preliminary assessment of image quality, with categorization of each image in one of three mutually exclusive quality categories (Good, Usable, Reject) based on the estimated probability of belonging to each class.[56] Only images rated as 'Good' or 'Usable' were retained; images classified as ‘Reject” were excluded.

Systemic biomarkers

The following laboratory biomarkers were included as outcome variables: glycated haemoglobin (HbA1c), serum creatinine, estimated glomerular filtration rate (eGFR), total cholesterol, high-density lipoprotein cholesterol (HDL-C), low-density lipoprotein cholesterol (LDL-C), serum triglycerides, urine creatinine, urine albumin, and urine albumin-to-creatinine ratio (ACR). These were selected to cover key dimensions of metabolic and end-organ function relevant to diabetes: glycaemic control, renal function, and lipid metabolism.

Complication variables

Three groups of systemic complications were considered in the relevant analyses: **Cardiovascular complications** (including Heart Disease, Stroke, Heart Failure, Cardiomyopathy, Myocardial Infarction, Ischaemic Heart Disease, Deep Vein Thrombosis, Transcatheter Aortic Valve Implantation, Coronary Artery Bypass Grafting, Coronary Artery Disease as noted in the practice clinical folders), **Kidney Disease** and **Neuropathies** (including peripheral neuropathy and neuralgia as reported in the clinical folders). All variables were coded as binary indicators (presence/absence).

Zone comparison (Zone B vs Zone C)

For each retinal parameter measured in both Zone B and Zone C, differences between zones were assessed using a paired-samples t-test, pairing observations from the same patient. The mean value in each zone, the absolute and percentage difference between zones, the t-statistic, and the corresponding p-value were recorded. Parameters with a significant difference ($p < 0.05$) between zones are reported.

Relationship between vascular parameters, biomarkers and complications

A series of linear regression models was fitted, with each of the systemic biomarkers as outcomes, one of the vascular parameters as a predictor and age, gender and image centering (central vs nasal) as covariates for basic confounding adjustment. Statistically significant ($P < 0.05$) regression coefficients for the main predictors are reported, together with scatter plots showing graphically the relationships between the parameters and the outcome.

Similarly, the association between vascular parameters and systemic diabetic complications was investigated by fitting a series of logistic regression models with the complications as binary outcomes, one of the vascular parameters as a predictor and

adjustment as above. Statistically significant odds ratios (OR) were reported for the main predictors .

In all models the vascular parameters were standardized for ease of comparisons, and a sandwich estimator was used to adjust the standard errors for the non-independence originating from the presence of multiple images for the same patient. In the estimation, data points were weighted with the squared values of the image quality coefficients (Automorph-estimated probability of good quality image). Given the exploratory nature of the analyses, no adjustment was considered for multiple comparisons.

Predictive model for chronic kidney disease

As a proof-of-concept predictive model for systemic diabetes complications we developed and assessed the performance of a model aimed at identifying patients with high risk of chronic kidney disease (CKD). We focus on the identification of early stages of CKD, defined as eGFR < 60 ml/min/1.73m2 and/or ACR ≥ 3 mg/mmol (Figure 5).

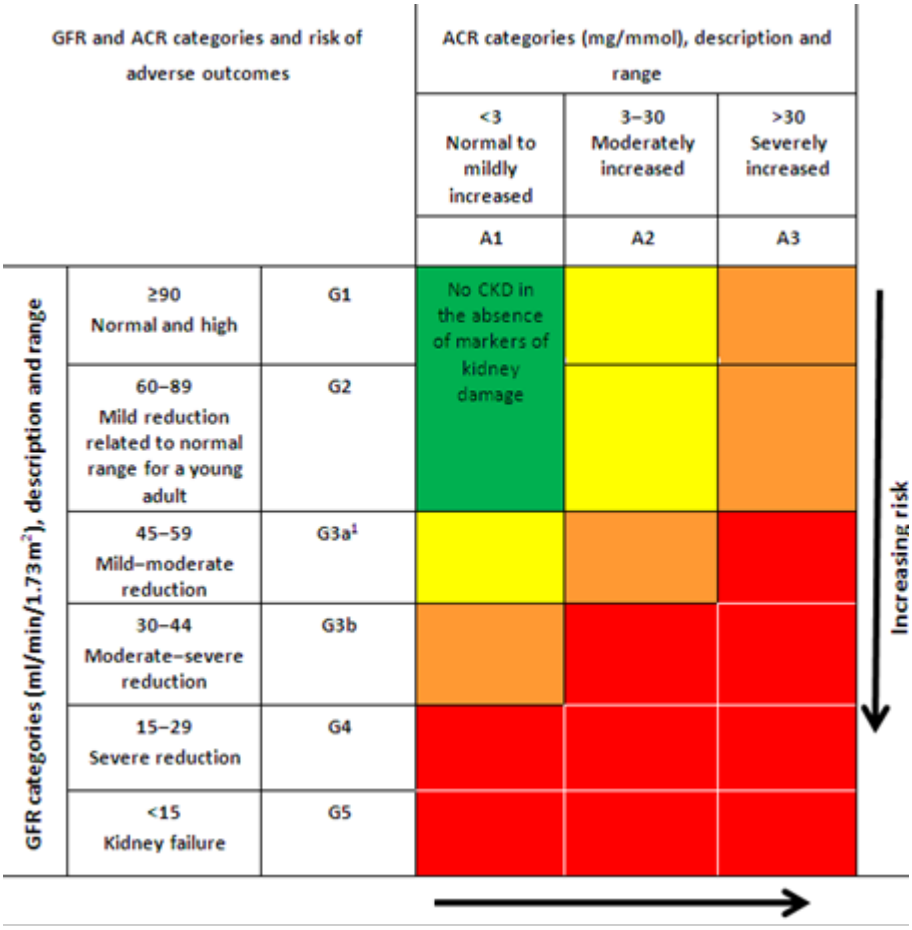

Figure adapted from [58]

Figure 5: Chronic Kidney Disease categories and risk of adverse outcomes

Modelling approach

We developed a deep learning–based binary image classification model in Python using the *PyTorch* deep learning framework and employed transfer learning with convolutional neural network (CNN) architectures pretrained on the ImageNet dataset.

Transfer learning was employed using pretrained CNN architectures available in the *Torchvision* library. The primary architecture used was EfficientNet-B0 with the original classification layer replaced with a custom binary classification head consisting of:

1. A dropout layer with dropout probability ($p = 0.2$)
2. A fully connected linear layer with a single output neuron

The final output represented the probability of kidney disease present.

Dataset preparation

Retinal fundus images were organized into training (80% of records) and validation (20%) datasets with corresponding binary labels representing the presence or absence of kidney disease as defined above. All images were converted to RGB format and resized to 224 x 224 pixels prior to model training. To improve model generalization and reduce overfitting, data augmentation techniques were applied to the training dataset. These augmentations included:

- Random horizontal and vertical flipping
- Random rotation up to 15°
- Colour jittering (brightness, contrast, saturation, and hue adjustments)
- Random affine transformations including translation and scaling

Following augmentation, images were converted to tensors and normalized using ImageNet mean and standard deviation values (μ= [0.485, 0.456, 0.406], σ = [0.229, 0.224, 0.225]).

Validation images underwent only resizing and normalization without augmentation.

Training strategy

We use a two-phase fine-tuning strategy:

1. Phase 1 – Classifier Head Training

The pretrained backbone was frozen, and only the classifier head was trained for 5 epochs using a learning rate of 10^{-3}.

2. Phase 2 – Full Model Fine-Tuning:

All network layers were unfrozen, and the entire model was fine-tuned for up to 45 additional epochs using a lower learning rate of 10^{-5}.

A *ReduceLROnPlateau* learning-rate scheduler was used to reduce the learning rate when validation performance plateaued.

Predictions were converted to binary outputs (presence/absence of outcome) using a classification threshold of 0.5. The best-performing model was selected based on validation AUC.

Early stopping was implemented with a patience value of 10 epochs to prevent overfitting. Model checkpoints corresponding to the highest validation AUC were saved during training.

Model evaluation

Model performance was evaluated on the validation dataset using the following metrics:

- Accuracy
- Precision
- Recall (Sensitivity)
- F1-score
- Area Under the Receiver Operating Characteristic Curve (AUC-ROC)

In order to quantify the uncertainty in the performance metrics, we repeated the entire process (training + evaluation) 50 times with random split between training and evaluation datasets, and summarised graphically and analytically the distribution of the various metrics.

Attention analyses

To improve the interpretability of the deep learning model and gain insights on the underlying mechanisms, Gradient-weighted Class Activation Mapping (Grad-CAM) was implemented to visualize image regions contributing most strongly to model predictions.

The Grad-CAM framework generated heatmaps highlighting retinal areas that influenced the classification of kidney disease from the images. For each input image, the trained convolutional neural network generated prediction probabilities and corresponding Grad-CAM activation maps. The Grad-CAM heatmaps represented the spatial distribution of model attention by highlighting regions with the highest contribution to the final prediction. The generated heatmaps were normalized to values between 0 and 1 and superimposed onto the original retinal fundus images to provide an interpretable overlay of the model's attention patterns.

To quantitatively analyse model attention, the retinal image was partitioned into five anatomical attention regions:

- Central region
- Quadrant 1 (top-right)

- Quadrant 2 (top-left)
- Quadrant 3 (bottom-left)
- Quadrant 4 (bottom-right)

The central region was defined using a circular mask centered on the image, while the remaining image area was divided into four quadrants using horizontal and vertical axes through the image centre. For each region, the proportion of Grad-CAM activation intensity was computed to quantify the distribution of model attention. The region receiving the highest activation score was identified as the primary focus region.

Anomaly detection

An experimental pipeline for the identification of vascular abnormalities was also implemented. The detector was designed to identify three categories of lesion: exudates, haemorrhages, and microaneurysms. Arteriole-venule (AV) nicking was included in the framework but was not activated in the current analysis due to algorithmic complexity. All processing steps were applied to the green channel of the RGB fundus image, which provides the highest contrast for retinal structures, except where colour information from additional channels was specifically required (haemorrhage detection).

Prior to lesion detection, each image underwent a standardised preprocessing pipeline. First, a binary mask delineating the valid fundus region was created to exclude the dark background periphery. The green channel was thresholded at an intensity of 10 to generate an initial foreground mask; morphological closing with an elliptical kernel (21 × 21 pixels) was then applied to fill internal holes. Only the largest connected component was retained, and the mask was eroded slightly (15 × 15 pixels) to eliminate edge artefacts. All subsequent processing was restricted to pixels within this fundus mask.

The green channel within the fundus region was then enhanced using Contrast Limited Adaptive Histogram Equalisation (CLAHE) with a clip limit of 1.5 and a tile grid size of 8 × 8. Background illumination variation was reduced by Gaussian unsharp masking: a Gaussian-blurred version of the enhanced image (σ = 15 pixels) was subtracted from the original with equal and opposite weights (factor 2.5 for both), yielding a locally normalised image centred on 128.

To minimise false positives arising from normal anatomical structures, the optic disc and retinal vessel network were identified and excluded from all lesion detection steps. The optic disc was detected by thresholding the green channel at an intensity of 180 to isolate bright regions, applying the fundus mask, and identifying connected components. The largest bright component was accepted as the optic disc if its area fell between 0.5% and 5% of the total image area (a range selected to correspond to the typical size of the optic disc across

fundus image resolutions). The resulting binary mask was dilated with an elliptical kernel scaled to 8% of the image width to create a conservative exclusion margin around the disc.

Retinal vessels were segmented using a multi-scale morphological black-hat transform applied to the CLAHE-enhanced green channel. Horizontal and vertical oriented rectangular structuring elements were applied at four scales (kernel lengths 5, 7, 9, and 11 pixels), and the resulting responses were summed to capture vessels of varying calibre. The combined vessel response image was normalised and thresholded at 15; small connected components smaller than 200 pixels were removed, and the remaining binary vessel map was dilated with a 5 × 5 elliptical kernel to ensure full coverage. The optic disc and vessel masks were combined into a single exclusion mask applied uniformly across all subsequent lesion detectors.

Exudates, which appear as bright lipid deposits in the retina, were detected using a morphological top-hat transform applied to the green channel with a 7 × 7 elliptical structuring element, which highlights bright structures smaller than the kernel relative to their local background. The resulting top-hat image was thresholded at an intensity of 40. The fundus and exclusion masks were applied to remove detections within the optic disc or along vessel borders, and objects smaller than 50 pixels were discarded. Each candidate region was characterised by three properties: (1) mean green-channel intensity, (2) circularity (computed as $4\pi \times \text{area} / \text{perimeter}^2$ from the region contour), and (3) area. A composite confidence score was computed as a weighted sum: 0.5 × normalised intensity score + 0.3 × circularity + 0.2 × normalised area score. Regions with a confidence score below the minimum threshold (set to 0.4) were excluded. Retained exudates were further classified as hard exudates (circularity > 0.65) or soft exudates (circularity ≤ 0.65). The maximum candidate area was capped at 5,000 pixels to exclude large artefacts.

Haemorrhages, which appear as dark, reddish lesions, were detected using a combined criterion incorporating both the morphological appearance and spectral colour properties of candidate regions. A black-hat transform with a 9 × 9 elliptical structuring element was applied to the green channel to enhance dark, localised regions. Red channel dominance was quantified for each pixel as the ratio of the red channel intensity to the green channel intensity (clipped to a maximum of 3.0). The black-hat response and red dominance map were multiplied to produce a combined response image that was thresholded at 20. After applying the fundus and exclusion masks, objects smaller than 80 pixels were removed. Each candidate haemorrhage was characterised by: (1) mean red-to-green channel ratio (red dominance score), (2) darkness score (1 minus the normalised mean green intensity), and (3) area. A confidence score was computed as 0.4 × red dominance score + 0.3 × darkness score + 0.3 × normalised area score. Candidates with confidence below 0.4 were excluded.

Accepted regions were classified as flame haemorrhages (aspect ratio > 2.5) or dot haemorrhages (aspect ratio ≤ 2.5). The maximum candidate area was capped at 5,000 pixels.

Microaneurysms appear as tiny, dark, circular spots. Detection was performed using a black-hat transform with a small (3 × 3) elliptical structuring element to enhance punctate dark spots, followed by thresholding at 15. After applying exclusion masks, connected component analysis was performed. Only components with an area between 8 and 150 pixels were considered, consistent with the expected size range of microaneurysms. Candidate regions were required to meet a strict circularity criterion: the circularity score ($4\pi \times \text{area} / \text{perimeter}^2$) was computed from the region contour and used directly as the confidence score. Only candidates with circularity ≥ 0.7 and confidence ≥ 0.4 were retained. This strict shape requirement was intended to reduce false positives from elongated vessel fragments.

Figure 6 depicts a graphical summary of the modelling strategy.

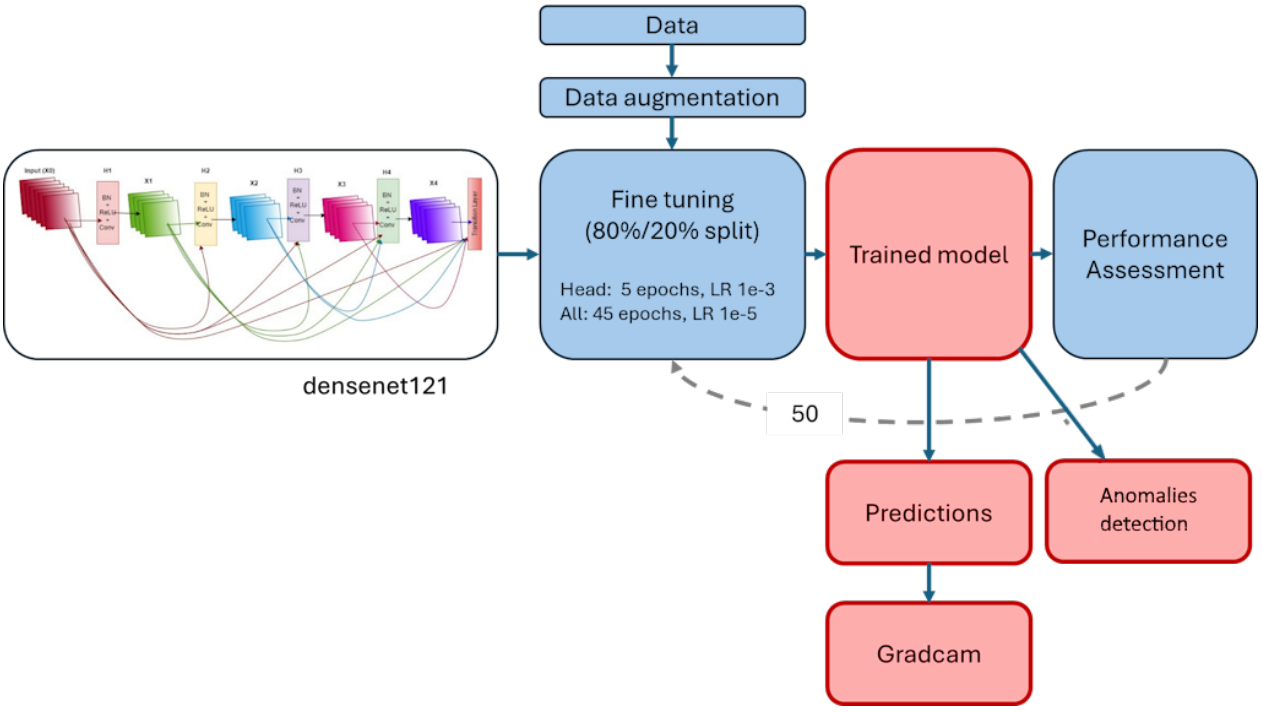

Figure 6: Predictive model for chronic kidney disease: strategy

Computation

All analyses were performed in Python (version 3.10) using the following libraries: *pandas* and *NumPy* for data management and array operations; *SciPy* for statistical tests (Spearman correlation, Mann-Whitney U, paired t-test, chi-squared distribution) and image processing

utilities; *scikit*-learn for linear and logistic regression, random forest modelling, and cross-validation; *OpenCV* for image input/output, morphological transforms, thresholding; *matplotlib* and *seaborn* for visualization.

Computations were run on a Linux machine with the following specifications:

- **OS**: *Ubuntu 24.04.3 LTS x86_64 (Kernel: 6.8.0-124-generic)*
- **Motherboard**: *Z790M AORUS ELITE*
- **CPU**: *Intel i7-14700K (28) @ 5.500GHz (20 cores)*
- **Memory**: *96 Gb*
- **GPU**: *NVIDIA GeForce RTX 5070 Ti, 16 Gb (Cuda version 13.0)*

Ethics

This study received ethics approval from the South African Medical Research Council Human Research Ethics Committee (Protocol ID: EC019-9/2024). All participants provided informed consent to provide information to the study.

RESULTS

Sample characteristics

Of the 320 adult diabetic patients who were screened for diabetic retinopathy in the first 2 years of implementation of the screening program, 200 (63%, 107 males and 93 females) responded to the invitation and provided informed consent to participate in the study. Their demographic and main clinical characteristics are summarised in Table 2.

Table 2: Sample characteristics

Characteristics	N	Females (N = 90)[1]	Males (N = 110)[1]
Demographics			
Age [Years]	200	52 (36, 60)	57 (45, 65)
Age category	200		
<25		6 (6.7%)	5 (4.5%)
25-34		14 (16%)	8 (7.3%)
35-44		17 (19%)	12 (11%)
45-54		16 (18%)	18 (16%)
55-64		23 (26%)	35 (32%)

Table 2: Sample characteristics

Characteristics	N	Females (N = 90)[1]	Males (N = 110)[1]
65-74		9 (10%)	22 (20%)
75+		5 (5.6%)	10 (9.1%)
Diabetes			
Type	200		
Type 2		51 (57%)	84 (76%)
Type 1		36 (40%)	25 (23%)
LADA		3 (3.3%)	1 (0.9%)
Duration [Years]	196		
<5		5 (5.7%)	13 (12%)
[5,10)		34 (39%)	23 (21%)
[10-15)		17 (19%)	22 (20%)
[15-20)		21 (24%)	26 (24%)
20+		11 (13%)	24 (22%)
Comorbidities			
Hypertension	200	59 (66%)	94 (85%)
Peripheral neuropathy	200	14 (16%)	39 (35%)
Kidney disease	200	7 (7.8%)	24 (22%)
Heart disease	200	1 (1.1%)	21 (19%)
Stroke	200	1 (1.1%)	8 (7.3%)
MAFLD	200	4 (4.4%)	0 (0%)
Treatment			
Insulin	200	69 (77%)	65 (59%)
Oral antidiabetic	200	50 (56%)	85 (77%)
GLP-1	200	12 (13%)	19 (17%)
Statins	200	49 (54%)	85 (77%)
Antihypertensives	200	47 (52%)	75 (68%)
Anthropometry & biomarkers			
Body Mass Index [Kg/m^2]	200	29.8 (25.0, 36.0)	29.1 (27.0, 32.0)
BMI Category	200		
Normal weight		20 (22%)	15 (14%)
Overweight		25 (28%)	46 (42%)
Obese I		20 (22%)	30 (27%)
Obese II		12 (13%)	13 (12%)
Obese III		13 (14%)	6 (5.5%)
Systolic Blood Pressure [mmHg]	200	134 (128, 145)	138 (130, 146)

Table 2: Sample characteristics

Characteristics	N	Females (N = 90)[1]	Males (N = 110)[1]
Diastolic Blood Pressure [mmHg]	200	85 (81, 92)	89 (83, 93)
HbA1c [%]	200	7.2 (6.5, 8.5)	7.1 (6.3, 7.9)
HbA1c < 7%	200	35 (39%)	48 (44%)
	Other		
Smoking	199		
Current		4 (4.5%)	13 (12%)
Former		3 (3.4%)	8 (7.3%)
Never		82 (92%)	89 (81%)

[1]Median (first quartile, third quartile); n (%)

LADA = Latent Autoimmune Diabetes in Adults; MAFLD = Metabolic dysfunction-associated fatty liver disease; GLP-I = Glucagon-Like Peptide-1; HbA1c = Glycated haemoglobin; BMI = Body Mass Index.

Participants were predominantly males (55%). Age ranged from 19 to 88 years (median 55 years, interquartile range 42 to 63 years). The majority of participants were diagnosed with type II diabetes (67%), which was especially frequent among men. Type I diabetes affected 30% of participants, and only 4 had a diagnosis of Latent Autoimmune Diabetes in Adults (LADA).

All participants had some form of comorbidity with other chronic diseases. Hypertension was the most common condition in both sexes. Other cardiovascular conditions (heart disease and stroke) were significantly more frequent among men. Peripheral neuropathy and kidney disease were the most reported complications. The large majority of patients were either overweight or obese according to the WHO cutoffs for Body Mass Index,[59] with only 22% of women and 14% of men in the normal weight range. Glycaemic control according to the cutoff commonly used in South Africa (HbA1c < 7%) was achieved by 39% of women and 44% of men. Only a minority of participants (8% of women and 21% of men) were current or past smokers.

Image quality

Of the 360 images in the female sample, 298 were classified as ‘Good’, 15 as ‘Usable’ and 47 excluded because of low quality. Of the 440 images in the male sample, 348 were classified as ‘Good’, 20 as ‘Usable’ and 72 of inadequate quality (Figure 7). In 4 cases (3

males and 1 female) all 4 images of a patient were deemed of insufficient quality, leading to the exclusion of the patient form the analyses. The total sample consisted, therefore of 89 females (with 313 images) and 107 males (368 images).

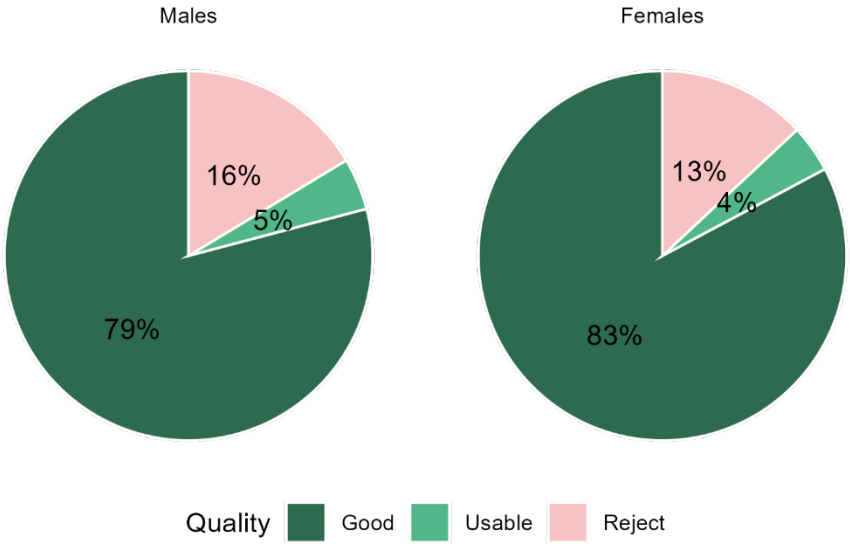

Figure 7: Image quality distribution, by gender

The quality of the images was affected by age, with a relatively stable probability of good quality until the age of 50, and a rapid decrease afterwards, more pronounced among women (-12%/decade) than men (-4.5%/decade). (Figure 8)

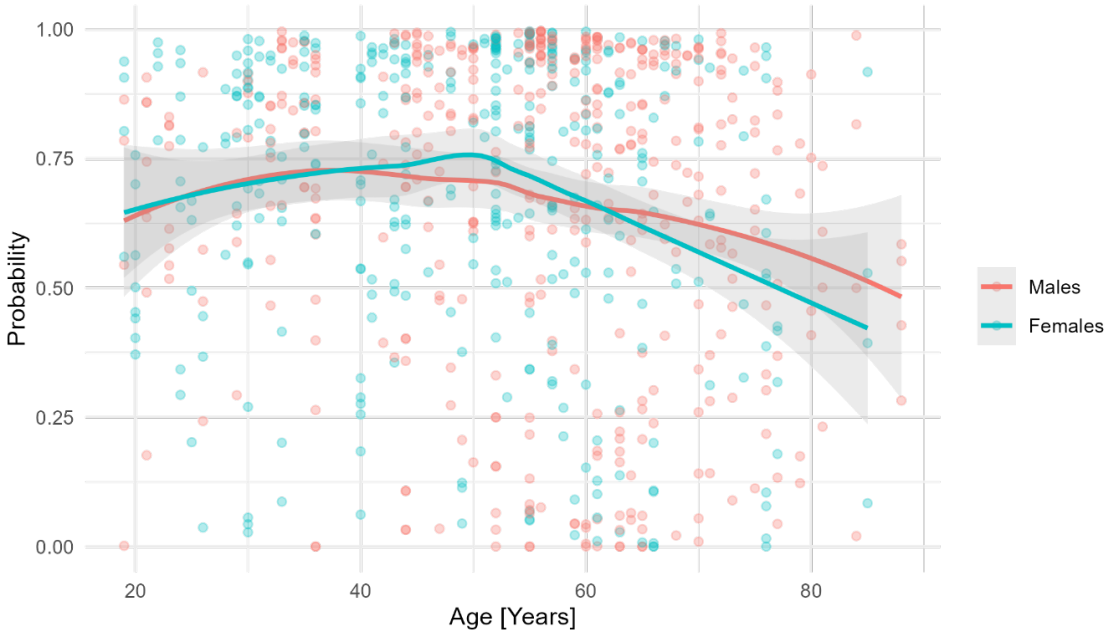

Figure 8: Probability of good image quality according to age, by gender.

Vascular features and clinical characteristics

On average, the between-zones differences in the vascular parameters were small in magnitude and in most cases not statistically significant (Figure 9).

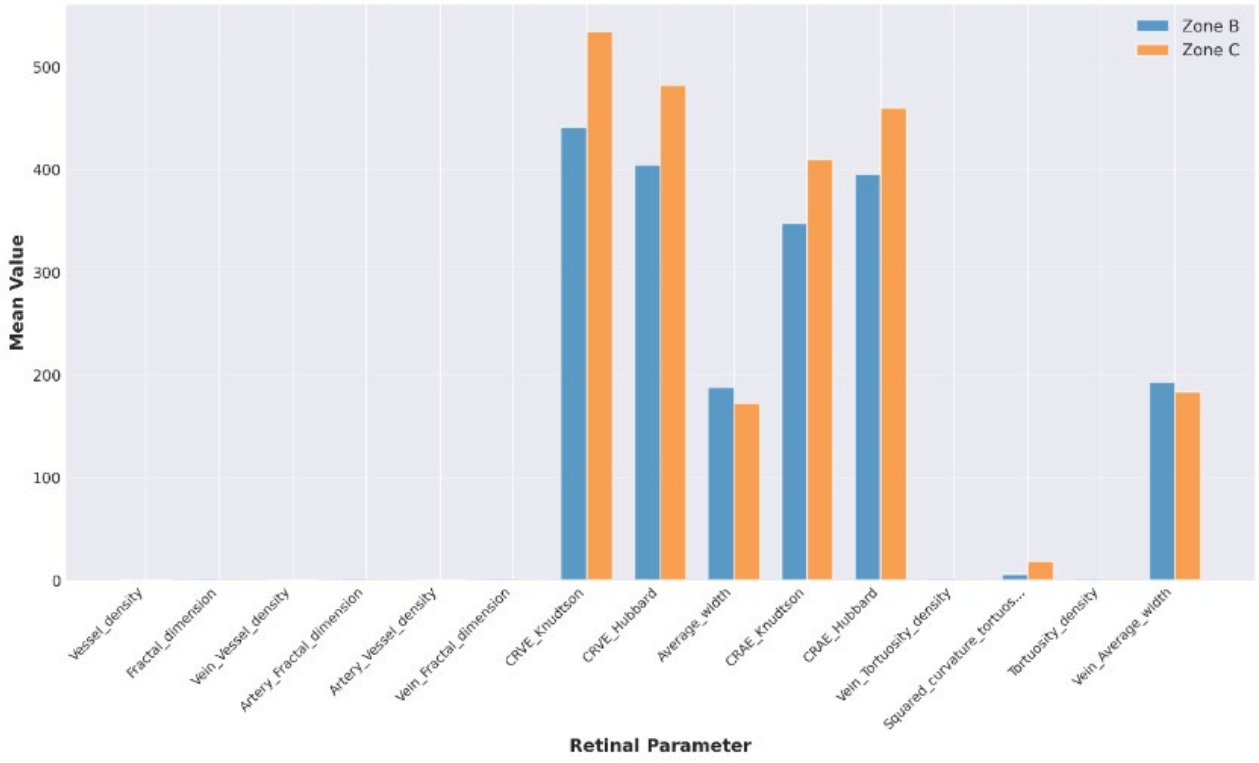

Figure 9: Average values of retinal parameters in Zone B vs Zone C. Significant differences.

The statistically significant relationships between vascular parameters and biomarkers are shown in Figure 10 and Table 3.

Biomarkers of reduced kidney function (low values of EGFR and high values of blood creatinine) are associated with high tortuosity and large calibres in the venular network (large average width and CVRE). Indicators of impaired lipid metabolism (high values of total and HDL cholesterol, low values of LDL cholesterol) are associated with high venular tortuosity and low artery calibre. Impaired glycaemic control (high values of HbA1c) is associated with reduced fractal dimension of both the venular and arterial network and sparseness of the arterial network.

Reduced kidney function, impaired lipid metabolism and impaired glycaemic control are, in turn, major risk factors for the development of kidney disease, cardiovascular disease and peripheral neuropathy (among other conditions), as summarised in Figure 11.

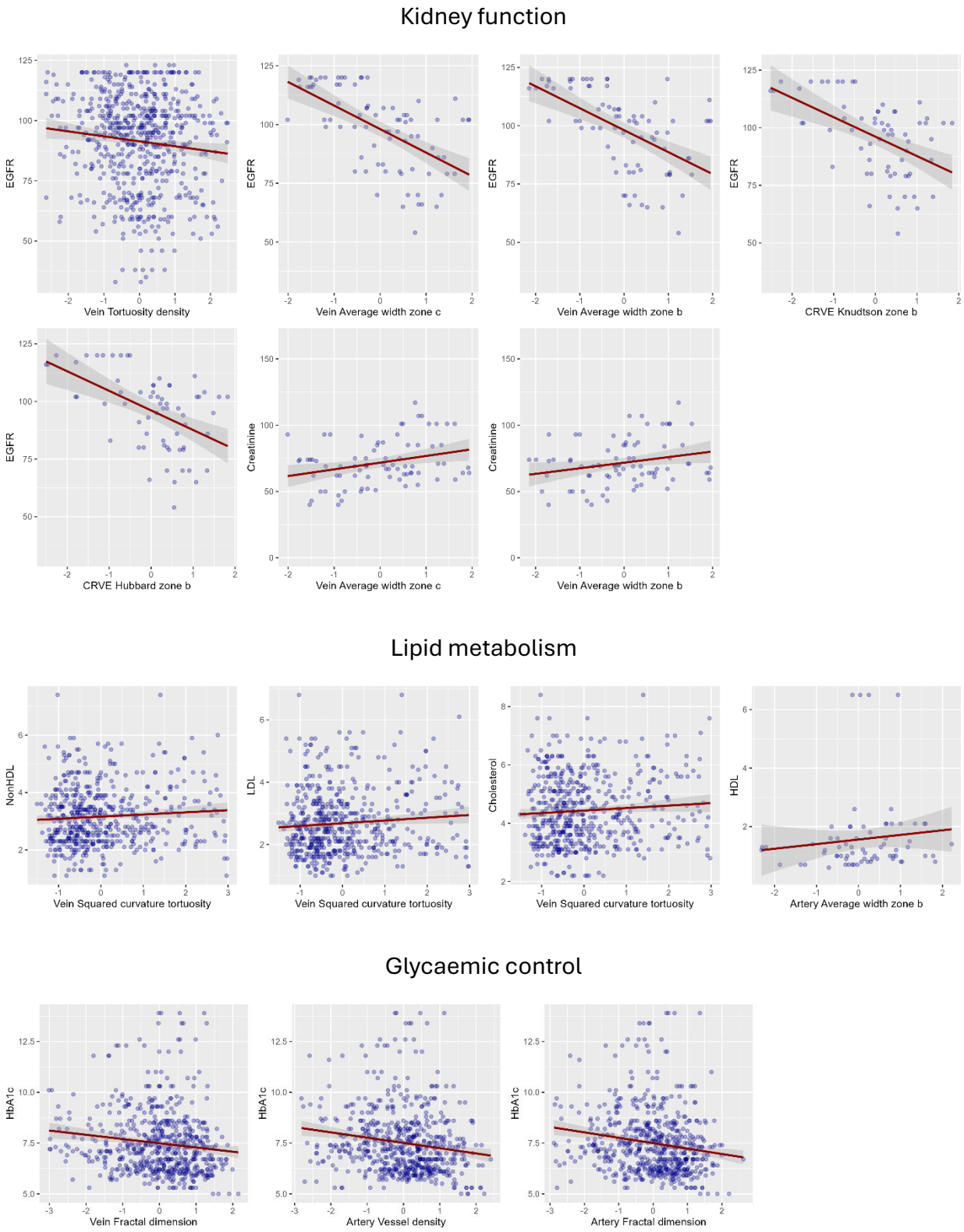

Only plots corresponding to statistically significant ($p < 0.05$) relationships are shown.

Figure 10: Relationships between retinal parameters and biomarkers.

Table 3: Relationships between vascular parameters and biomarkers

Vascular parameter	Biomarker	Regression coefficient	p-value
Artery Average width zone b	HDL	0.30	0.04
Artery Fractal dimension	HbA1c	-0.35	0.00
Artery Vessel density	HbA1c	-0.28	0.01
CRVE Hubbard zone b	eGFR	-5.69	0.05
CRVE Knudtson zone b	eGFR	-5.75	0.04
Vein Average width zone b	eGFR	-6.57	0.00
Vein Average width zone b	Blood Creatinine	5.71	0.01
Vein Average width zone c	eGFR	-6.03	0.02
Vein Average width zone c	Blood Creatinine	5.66	0.02
Vein Fractal dimension	HbA1c	-0.26	0.01
Vein Squared curvature tortuosity	NonHDL	0.12	0.03
Vein Squared curvature tortuosity	LDL	0.12	0.01
Vein Squared curvature tortuosity	Total Cholesterol	0.11	0.05
Vein Tortuosity density	eGFR	-1.32	0.04

Only statistically significant ($p < 0.05$) coefficients shown. Adjustment for age, gender and centering of retinal images.

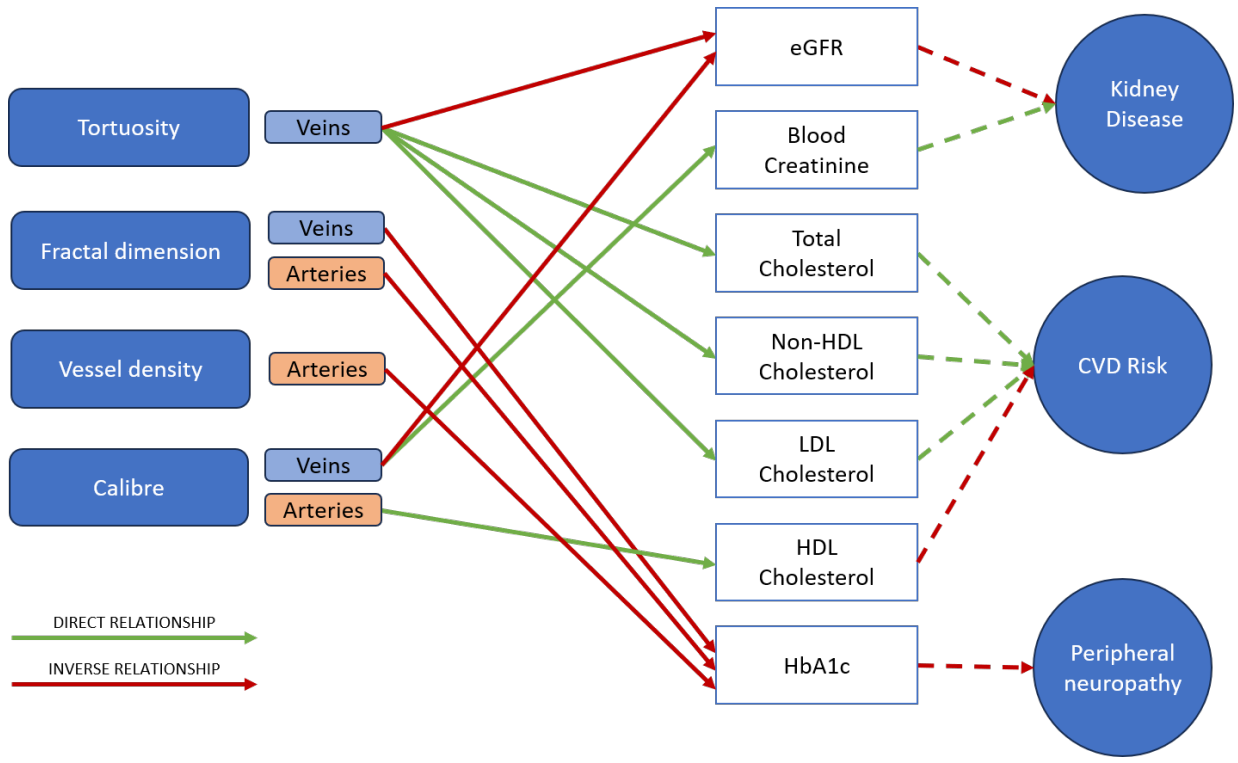

Figure 11: Summary of relationships between retinal parameters and biomarkers.

Finally, Table 4 summarises the relationships between retinal parameters and major clinically diagnosed classes of diabetic complications considered as binary variables (present vs absent).

Table 4: Relationship between vascular parameters and diabetic complications

		Odds Ratio		
Vascular parameter	**Complication**	**OR**	**lb**	**ub**
Artery Squared curvature tortuosity zone c	Cardiovascular	2.92	1.59	5.39
Vein Tortuosity density zone c	Cardiovascular	8.65	1.82	41.11
Artery Tortuosity density	Cardiovascular	0.66	0.48	0.9
Artery Average width	Cardiovascular	0.61	0.38	0.98
Vein Average width zone c	Neuropathy	6.8	1.71	27.02
Vein Average width zone b	Neuropathy	5.99	1.39	25.89
Vein Average width zone b	Kidney	0.2	0.05	0.77
Artery Tortuosity density	Kidney	0.68	0.49	0.95

As expected form the results of previous studies, and in agreement with the hypothesized mediating role of the biomarker in Figure 11, low tortuosity of both the venular and arterial network (artery squared curvature tortuosity zone c, vein tortuosity density zone c) and large calibres in the arterial network (artery average width) showed a protective effect on cardiovascular diseases, and wider veins (vein average width zone b and c) width were associated with increases odds of peripheral neuropathy.

The apparent protective effect on cardiovascular and kidney disease of increased tortuosity when measured on the whole vessel network with distinction between veins and artery (artery tortuosity density) is, however, contradictory, with a possible explanation being the fact that calculation over the whole image (rather than on specific zone) might have been affected by differences if the retinal areas included in the various images.

The overall protective effect of large venular calibres on kidney disease, finally, is not necessarily in contradiction with the harmful effects of large veins on both eGFR and blood creatinine, as the relationship between venular calibre and kidney disease is quite complex. Wider retinal venules are frequently associated with systematic inflammation, endothelial dysfunction, and a higher risk of incident kidney disease, and, in diabetic populations, widening of the retinal veins often precedes the clinical onset of diabetic nephropathy and strongly predicts subsequent proteinuria.[60,61] However, some clinical cohorts demonstrate significant narrowing of venules in patients with advanced chronic kidney disease, as result of structural remodelling and decreased blood flow as renal function deteriorates.[62] An

inverse relationship between venular calibre and kidney disease can be the result of advanced stages of disease in our sample.

Proof of concept screening model for chronic kidney disease

Table 5 and Figure 12 shows the results of the Montecarlo validation of the deep-learning screening model for early stages of chronic kidney disease.

The model, unsurprisingly given the limited size of the training sample, shows modest performances, with an area under the ROC curve of 0.73, an accuracy of 62%.

Table 5: *Performance metrics for the screening model*

Metric	Mean	Standard Deviation	Coefficient of variation (%)	Min	Max	Median
Accuracy	0.62	0.10	15.70	0.36	0.76	0.63
Precision	0.32	0.10	31.78	0.06	0.55	0.32
Recall	0.77	0.16	20.78	0.33	1.00	0.75
F1	0.43	0.10	23.96	0.11	0.61	0.45
AUC	0.73	0.07	9.62	0.54	0.85	0.73

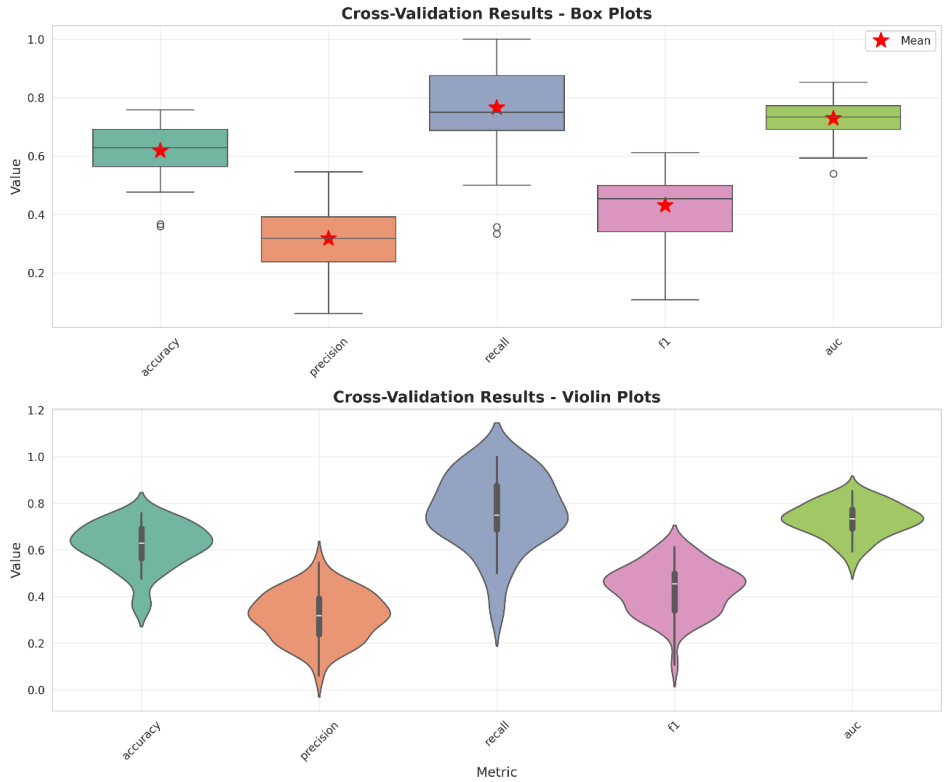

Figure 12: Performance metrics for the screening model

Figure 13 to Figure 17 show some examples of the attention analysis and anomaly detection.

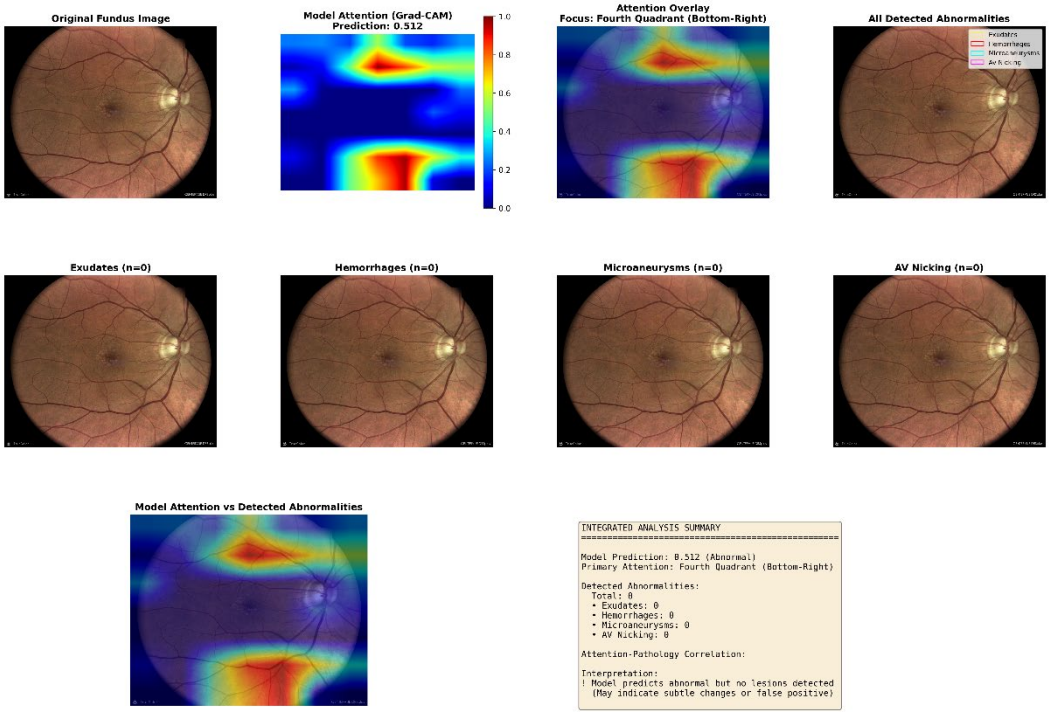

Figure 13: Attention analysis and anomaly detection: Patient 50, Right Eye, central

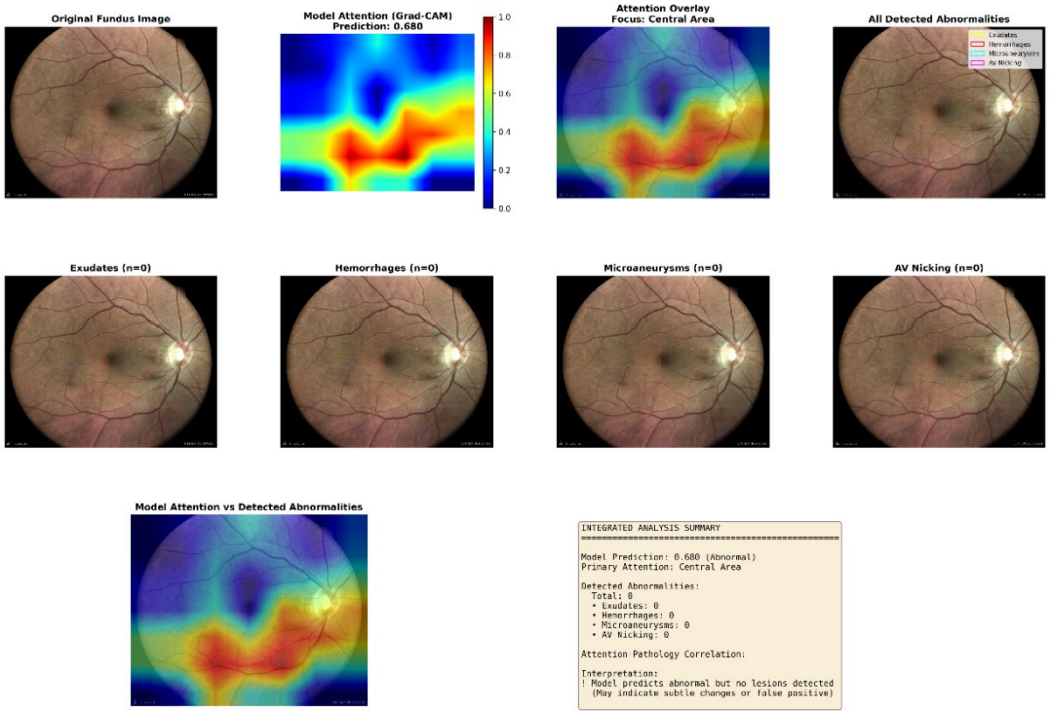

Figure 14: Attention analysis and anomaly detection: Patient 82, Right Eye, central

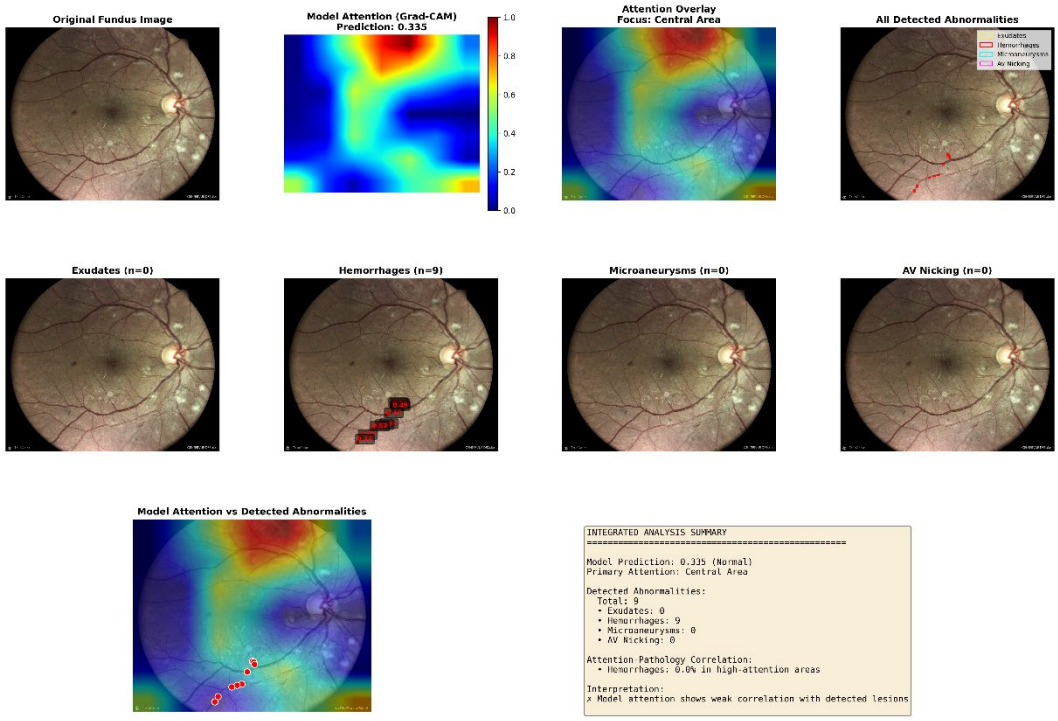

Figure 15: Attention analysis and anomaly detection: Patient 51, Right Eye, central

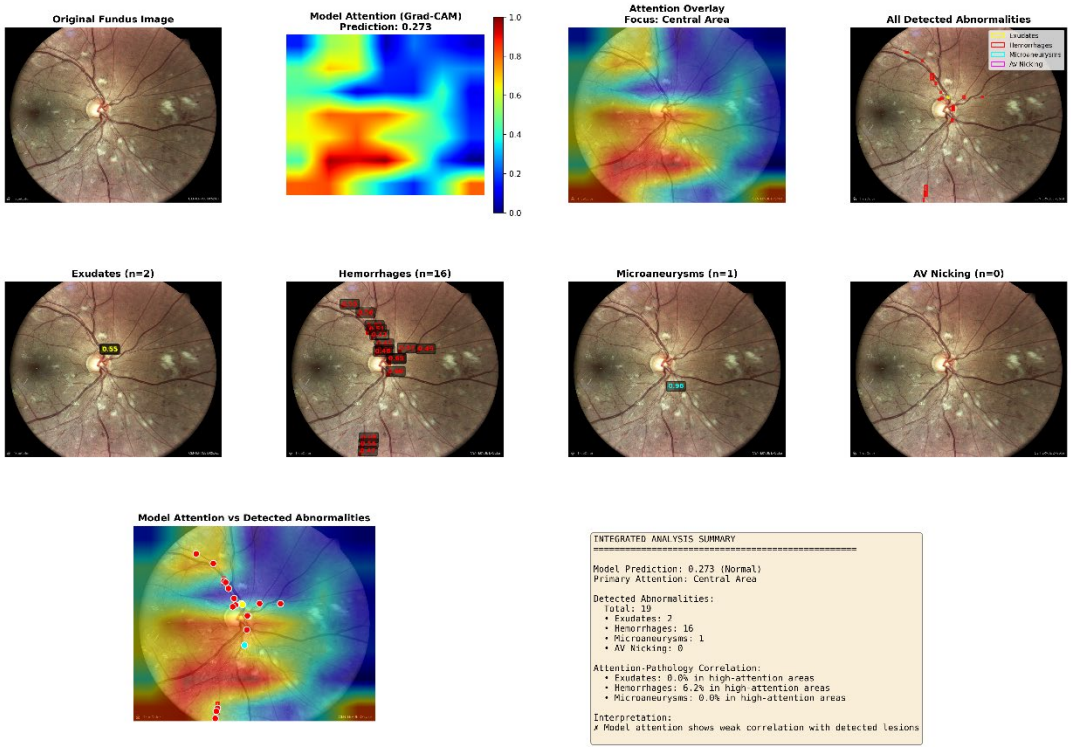

Figure 16: Attention analysis and anomaly detection: Patient 51, Right Eye, nasal

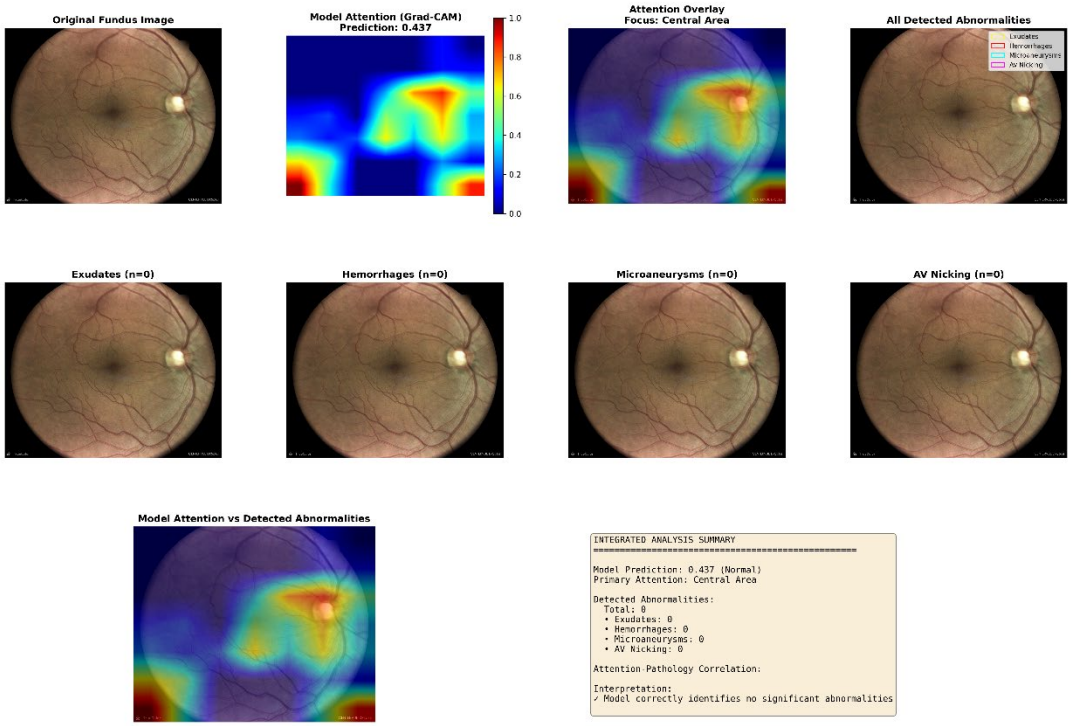

Figure 17: Attention analysis and anomaly detection: Patient 121, Right Eye, nasal

DISCUSSION AND CONCLUSION

This exploratory study investigated whether quantitative retinal vascular features extracted from fundus photographs could provide clinically relevant information regarding systemic vascular risk and diabetic complications. The findings contribute to the rapidly expanding field of oculomics, which proposes that the retinal microvasculature represents a visible and measurable extension of the systemic vascular system and may therefore offer insight into cardiovascular, renal, and metabolic disease processes.

The study identified several statistically significant relationships between retinal vascular morphology and biomarkers of diabetic disease severity. In particular, reduced renal function was associated with wider venular calibre and increased venular tortuosity. These findings are broadly consistent with previous studies demonstrating associations between retinal venular widening, endothelial dysfunction, systemic inflammation, and chronic kidney disease progression.[60–64] The observed relationships may reflect shared microvascular pathological mechanisms affecting both the retinal and renal circulations, including oxidative stress, chronic inflammation, and impaired endothelial autoregulation.

Poor glycaemic control, reflected by elevated HbA1c levels, was associated with lower fractal dimension and reduced vessel density. Reduced fractal dimension has previously been interpreted as evidence of microvascular rarefaction and loss of vascular branching complexity in diabetic populations. These findings are biologically plausible because chronic hyperglycaemia contributes to capillary dropout, vascular remodelling, and impaired angiogenic regulation. Similar associations between retinal vascular complexity and diabetes severity have been reported in prior oculomics and retinal vascular studies.[42,48,65,66]

The observed relationships between retinal vascular parameters and clinically diagnosed complications further support the hypothesis that retinal morphology may reflect broader systemic vascular dysfunction. Wider venular calibre was associated with peripheral neuropathy, while selected measures of tortuosity and arterial calibre were associated with cardiovascular disease. These findings align with the broader literature demonstrating links between retinal microvascular abnormalities and cardiovascular outcomes, stroke, and all-cause mortality in patients with diabetes.[67–69]

At the same time, several findings require cautious interpretation. Some apparently protective associations involving tortuosity and kidney disease were inconsistent with established pathophysiological expectations. These discrepancies may reflect the complexity of retinal vascular remodelling across different stages of chronic disease, but they may also arise from methodological limitations, including variability in image regions analysed, residual confounding, or instability related to the relatively small sample size. Because this study was exploratory and hypothesis-generating, no correction for multiple testing was applied, increasing the possibility that some statistically significant findings may represent chance associations.

A contribution of the study was the development of a proof-of-concept deep learning model for chronic kidney disease screening from retinal images. Although predictive performance was moderate, the model achieved a mean AUC of 0.73 despite being trained on a relatively limited dataset collected in routine clinical practice rather than highly standardised research settings. These findings are encouraging because most existing AI models for systemic disease prediction have been developed using large curated datasets under tightly controlled imaging conditions, which may limit their generalisability to real-world healthcare environments.

The use of Grad-CAM attention analysis represents a further strength of the study because it partially addresses concerns regarding the “black-box” nature of deep learning systems. The

attention maps suggested that the model focused predominantly on vascular and anatomically plausible retinal regions when generating predictions, supporting the biological credibility of the learned features. Explainability remains critically important for the future implementation of AI-assisted decision support systems in clinical medicine, particularly in high-risk conditions such as diabetic vascular disease.

The study also demonstrates the practical feasibility of implementing AI-supported retinal imaging workflows in South African clinical settings. The use of non-mydriatic cameras operated by trained non-specialists and integrated into routine diabetic consultations reflects a potentially scalable approach to diabetic screening and risk stratification. In resource-constrained health systems, retinal imaging could eventually function as a rapid, non-invasive adjunct screening tool capable of identifying patients who require further laboratory or specialist assessment.

Several limitations should be acknowledged. First, the cross-sectional nature of the analyses prevents causal inference and limits conclusions regarding temporal relationships between retinal changes and systemic disease progression. Second, the sample size was modest and derived from a single specialist practice, which may limit generalisability. Third, although image quality assessment and weighting procedures were implemented, image quality variability remains an important source of measurement error in real-world retinal imaging studies. Fourth, comorbidity data were extracted from routine clinical records and may be affected by incomplete documentation or diagnostic heterogeneity. Finally, the exploratory analytical strategy involved numerous statistical tests without formal multiplicity adjustment, meaning that findings should be interpreted primarily as hypothesis-generating.

Despite these limitations, the study provides valuable preliminary evidence supporting the potential role of retinal imaging and AI-assisted vascular analysis in systemic disease stratification among patients with diabetes. The findings reinforce the concept that retinal microvascular alterations may serve as accessible biomarkers of broader vascular dysfunction and systemic disease burden.

Future work should focus on validating these findings in larger and more diverse cohorts, including longitudinal designs capable of evaluating the predictive value of retinal biomarkers for future disease outcomes. Further refinement of machine learning models, harmonisation across imaging platforms, and integration with conventional clinical and laboratory risk markers may substantially improve predictive performance. The continued development of explainable and clinically interpretable AI systems will also be essential before widespread implementation can occur.

In conclusion, this exploratory study demonstrates that AI-based analysis of retinal fundus images can identify meaningful associations between retinal vascular morphology and systemic diabetic complications, while also supporting the feasibility of proof-of-concept predictive modelling for chronic kidney disease. Although additional validation is required, the findings contribute to the growing evidence that retinal imaging may become an important component of future precision medicine and vascular risk stratification strategies in diabetes care.

REFERENCES

1. Damaskos C, Garmpis N, Kollia P, et al. Assessing Cardiovascular Risk in Patients with Diabetes: An Update. *Curr Cardiol Rev*. 2020;16(4):266-274. doi:10.2174/1573403X15666191111123622

2. Li Y, Liu Y, Liu S, et al. Diabetic vascular diseases: molecular mechanisms and therapeutic strategies. *Sig Transduct Target Ther*. 2023;8(1):1-29. doi:10.1038/s41392-023-01400-z

3. Creager MA, Lüscher TF, prepared with the assistance of, Cosentino F, Beckman JA. Diabetes and Vascular Disease. *Circulation*. 2003;108(12):1527-1532. doi:10.1161/01.CIR.0000091257.27563.32

4. Jönsson B, CODE-2 Advisory Board. Revealing the cost of Type II diabetes in Europe. *Diabetologia*. 2002;45(7):S5-12. doi:10.1007/s00125-002-0858-x

5. Marshall SM, Flyvbjerg A. Prevention and early detection of vascular complications of diabetes. *BMJ*. 2006;333(7566):475-480. doi:10.1136/bmj.38922.650521.80

6. Opperman A, De Klerk M. A total cost perspective of type 1 and 2 diabetes mellitus in two South African medical schemes servicing the public healthcare sector. *South African Medical Journal*. 2021;111(7):635-641.

7. Pham TB, Nguyen TT, Truong HT, et al. Effects of Diabetic Complications on Health-Related Quality of Life Impairment in Vietnamese Patients with Type 2 Diabetes. *J Diabetes Res*. 2020;2020:4360804. doi:10.1155/2020/4360804

8. Al-Abadla Z, Elgzyri T, Moussa M. The Effect of Diabetes on Health-Related Quality of Life in Emirati Patients. *Dubai Diabetes and Endocrinology Journal*. 2022;28(1):35-44. doi:10.1159/000520599

9. Janssen LMM, Hiligsmann M, Elissen AMJ, et al. Burden of disease of type 2 diabetes mellitus: cost of illness and quality of life estimated using the Maastricht Study. *Diabet Med*. 2020;37(10):1759-1765. doi:10.1111/dme.14285

10. Cheung N, Mitchell P, Wong TY. Diabetic retinopathy. *The Lancet*. 2010;376(9735):124-136. doi:10.1016/S0140-6736(09)62124-3

11. Klein BEK. Overview of epidemiologic studies of diabetic retinopathy. *Ophthalmic Epidemiol*. 2007;14(4):179-183. doi:10.1080/09286580701396720

12. Ting DSW, Cheung GCM, Wong TY. Diabetic retinopathy: global prevalence, major risk factors, screening practices and public health challenges: a review. *Clinical & Experimental Ophthalmology*. 2016;44(4):260-277. doi:10.1111/ceo.12696

13. Bourne RRA, Stevens GA, White RA, et al. Causes of vision loss worldwide, 1990-2010: a systematic analysis. *Lancet Glob Health*. 2013;1(6):e339-349. doi:10.1016/S2214-109X(13)70113-X

14. Yau JWY, Rogers SL, Kawasaki R, et al. Global prevalence and major risk factors of diabetic retinopathy. *Diabetes Care*. 2012;35(3):556-564. doi:10.2337/dc11-1909

15. Gross JL, de Azevedo MJ, Silveiro SP, Canani LH, Caramori ML, Zelmanovitz T. Diabetic Nephropathy: Diagnosis, Prevention, and Treatment. *Diabetes Care*. 2005;28(1):164-176. doi:10.2337/diacare.28.1.164

16. Fowler MJ. Microvascular and Macrovascular Complications of Diabetes. *Clinical Diabetes*. 2008;26(2):77-82. doi:10.2337/diaclin.26.2.77

17. Nathan DM, Meigs J, Singer DE. The epidemiology of cardiovascular disease in type 2 diabetes mellitus: how sweet it is ... or is it? *The Lancet*. 1997;350:S4-S9. doi:10.1016/S0140-6736(97)90021-0

18. Laing SP, Swerdlow AJ, Slater SD, et al. Mortality from heart disease in a cohort of 23,000 patients with insulin-treated diabetes. *Diabetologia*. 2003;46(6):760-765. doi:10.1007/s00125-003-1116-6

19. Kannel WB, McGee DL. Diabetes and cardiovascular disease. The Framingham study. *JAMA*. 1979;241(19):2035-2038. doi:10.1001/jama.241.19.2035

20. Wong ND, Sattar N. Cardiovascular risk in diabetes mellitus: epidemiology, assessment and prevention. *Nat Rev Cardiol*. 2023;20(10):685-695. doi:10.1038/s41569-023-00877-z

21. The Emerging Risk Factors CollaborationCollaboration. Diabetes mellitus, fasting blood glucose concentration, and risk of vascular disease: a collaborative meta-analysis of 102 prospective studies. *The Lancet*. 2010;375(9733):2215-2222. doi:10.1016/S0140-6736(10)60484-9

22. Saraste A, Knuuti J, Bax J. Screening for Coronary Artery Disease in Patients with Diabetes. *Curr Cardiol Rep*. 2023;25(12):1865-1871. doi:10.1007/s11886-023-01999-z

23. The Diabetes Control and Complications Trial Research Group. The Effect of Intensive Treatment of Diabetes on the Development and Progression of Long-Term Complications in Insulin-Dependent Diabetes Mellitus. *New England Journal of Medicine*. 1993;329(14):977-986. doi:10.1056/NEJM199309303291401

24. American Diabetes Association Professional Practice Committee. 4. Comprehensive Medical Evaluation and Assessment of Comorbidities: Standards of Care in Diabetes—2024. *Diabetes Care*. 2023;47(Supplement_1):S52-S76. doi:10.2337/dc24-S004

25. McGuire H, Longson D, Adler A, Farmer A, Lewin I. Management of type 2 diabetes in adults: summary of updated NICE guidance. *Bmj*. 2016;353.

26. Aschner P. New IDF clinical practice recommendations for managing type 2 diabetes in primary care. *Diabetes research and clinical practice*. 2017;132:169-170.

27. Nicolaou V, Huddle K. SEMDSA 2017 guidelines for the management of type 2 diabetes mellitus. *J Endocrinol Metab Diabetes S Afr*. 2017;22(1 Suppl 1):S1-S196.

28. Morello CM. Etiology and natural history of diabetic retinopathy: An overview. *American Journal of Health-System Pharmacy*. 2007;64(17_Supplement_12):S3-S7. doi:10.2146/ajhp070330

29. Mansour SE, Browning DJ, Wong K, Flynn Jr HW, Bhavsar AR. The Evolving Treatment of Diabetic Retinopathy. *Clinical Ophthalmology*. 2020;14:653-678. doi:10.2147/OPTH.S236637

30. World Health Organization. Screening programmes: a short guide. Increase effectiveness, maximize benefits and minimize harm. Published online 2020.

31. Li Z, Keel S, Liu C, et al. An automated grading system for detection of vision-threatening referable diabetic retinopathy on the basis of color fundus photographs. *Diabetes care*. 2018;41(12):2509-2516.

32. EyRIS - Screen For Life. Accessed March 1, 2023. https://www.screenforlife.co.za/EyRIS

33. Bellemo V, Lim ZW, Lim G, et al. Artificial intelligence using deep learning to screen for referable and vision-threatening diabetic retinopathy in Africa: a clinical validation study. *Lancet Digit Health*. 2019;1(1):e35-e44. doi:10.1016/S2589-7500(19)30004-4

34. Nørgaard MF, Grauslund J. Automated Screening for Diabetic Retinopathy – A Systematic Review. *ORE*. 2018;60(1):9-17. doi:10.1159/000486284

35. Mathenge WC. Artificial intelligence for diabetic retinopathy screening in Africa. *The Lancet Digital Health*. 2019;1(1):e6-e7. doi:10.1016/S2589-7500(19)30009-3

36. Wawer Matos PA, Reimer RP, Rokohl AC, Caldeira L, Heindl LM, Große Hokamp N. Artificial Intelligence in Ophthalmology - Status Quo and Future Perspectives. *Semin Ophthalmol*. 2023;38(3):226-237. doi:10.1080/08820538.2022.2139625

37. Ipp E, Liljenquist D, Bode B, et al. Pivotal Evaluation of an Artificial Intelligence System for Autonomous Detection of Referrable and Vision-Threatening Diabetic Retinopathy. *JAMA Netw Open*. 2021;4(11):e2134254. doi:10.1001/jamanetworkopen.2021.34254

38. Barrot J, Real J, Vlacho B, et al. Diabetic retinopathy as a predictor of cardiovascular morbidity and mortality in subjects with type 2 diabetes. *Front Med*. 2022;9. doi:10.3389/fmed.2022.945245

39. Hägg S, Thorn LM, Putaala J, et al. Incidence of Stroke According to Presence of Diabetic Nephropathy and Severe Diabetic Retinopathy in Patients With Type 1 Diabetes. *Diabetes Care*. 2013;36(12):4140-4146. doi:10.2337/dc13-0669

40. Ong YT, De Silva DA, Cheung CY, et al. Microvascular Structure and Network in the Retina of Patients With Ischemic Stroke. *Stroke*. 2013;44(8):2121-2127. doi:10.1161/STROKEAHA.113.001741

41. Mordi IR, Trucco E, Syed MG, et al. Prediction of Major Adverse Cardiovascular Events From Retinal, Clinical, and Genomic Data in Individuals With Type 2 Diabetes: A Population Cohort Study. *Diabetes Care*. 2022;45(3):710-716. doi:10.2337/dc21-1124

42. Cabrera DeBuc D, Somfai GM, Koller A. Retinal microvascular network alterations: potential biomarkers of cerebrovascular and neural diseases. *American Journal of Physiology-Heart and Circulatory Physiology*. 2017;312(2):H201-H212. doi:10.1152/ajpheart.00201.2016

43. Petitti DB, Bhatt H. Retinopathy as a Risk Factor for Nonembolic Stroke in Diabetic Subjects. *Stroke*. 1995;26(4):593-596. doi:10.1161/01.STR.26.4.593

44. Abdollahi M, Jafarizadeh A, Asbagh AG, et al. Artificial Intelligence in Assessing Cardiovascular Diseases and Risk Factors via Retinal Fundus Images: A Review of the Last Decade. *arXiv*. Preprint posted online November 11, 2023:arXiv:2311.07609. doi:10.48550/arXiv.2311.07609

45. Chikumba S, Hu Y, Luo J. Deep learning-based fundus image analysis for cardiovascular disease: a review. *Therapeutic Advances in Chronic Disease*. 2023;14:20406223231209895. doi:10.1177/20406223231209895

46. Wagner SK, Fu DJ, Faes L, et al. Insights into Systemic Disease through Retinal Imaging-Based Oculomics. *Transl Vis Sci Technol*. 9(2):6. doi:10.1167/tvst.9.2.6

47. Arnould L, Guenancia C, Bourredjem A, et al. Prediction of Cardiovascular Parameters With Supervised Machine Learning From Singapore “I” Vessel Assessment and OCT-

Angiography: A Pilot Study. *Transl Vis Sci Technol*. 2021;10(13):20. doi:10.1167/tvst.10.13.20

48. Wong TY, Klein R, Klein BE, Tielsch JM, Hubbard L, Nieto FJ. Retinal microvascular abnormalities and their relationship with hypertension, cardiovascular disease, and mortality. *Surv Ophthalmol*. 2001;46(1):59-80. doi:10.1016/s0039-6257(01)00234-x

49. Jeba Sheela A, Krishnamurthy M. Revolutionizing cardiovascular risk prediction: A novel image-based approach using fundus analysis and deep learning. *Biomedical Signal Processing and Control*. 2024;90:105781. doi:10.1016/j.bspc.2023.105781

50. Arnould L, Meriaudeau F, Guenancia C, et al. Using Artificial Intelligence to Analyse the Retinal Vascular Network: The Future of Cardiovascular Risk Assessment Based on Oculomics? A Narrative Review. *Ophthalmol Ther*. 2023;12(2):657-674. doi:10.1007/s40123-022-00641-5

51. D'Agostino RB, Vasan RS, Pencina MJ, et al. General Cardiovascular Risk Profile for Use in Primary Care. *Circulation*. 2008;117(6):743-753. doi:10.1161/CIRCULATIONAHA.107.699579

52. World Health Organization. Hearts: technical package for cardiovascular disease management in primary health care. Published online 2020.

53. Gijsberts CM, Groenewegen KA, Hoefer IE, et al. Race/Ethnic Differences in the Associations of the Framingham Risk Factors with Carotid IMT and Cardiovascular Events. *PLOS ONE*. 2015;10(7):e0132321. doi:10.1371/journal.pone.0132321

54. Yeboah J, McClelland RL, Polonsky TS, et al. Comparison of Novel Risk Markers for Improvement in Cardiovascular Risk Assessment in Intermediate Risk Individuals. The Multi-Ethnic Study of Atherosclerosis. *JAMA*. 2012;308(8):788-795. doi:10.1001/jama.2012.9624

55. Patterson EJ, Bounds AD, Wagner SK, Kadri-Langford R, Taylor R, Daly D. Oculomics: A Crusade Against the Four Horsemen of Chronic Disease. *Ophthalmol Ther*. 2024;13(6):1427-1451. doi:10.1007/s40123-024-00942-x

56. Zhou Y, Wagner SK, Chia MA, et al. AutoMorph: Automated Retinal Vascular Morphology Quantification Via a Deep Learning Pipeline. *Translational Vision Science & Technology*. 2022;11(7):12. doi:10.1167/tvst.11.7.12

57. Gao Y, Xu L, He N, et al. A narrative review of retinal vascular parameters and the applications (Part I): Measuring methods. *Brain Circ*. 2023;9(3):121-128. doi:10.4103/bc.bc_8_23

58. Levin A, Stevens PE, Bilous RW, et al. Kidney disease: Improving global outcomes (KDIGO) CKD work group. KDIGO 2012 clinical practice guideline for the evaluation and

management of chronic kidney disease. *Kidney International Supplements*. 2013;3(1):1-150. doi:10.1038/kisup.2012.73

59. WHO Consultation on Obesity (1999: Geneva S, Organization WH. *Obesity : preventing and managing the global epidemic : report of a WHO consultation*. World Health Organization; 2000. Accessed July 22, 2025. https://iris.who.int/handle/10665/42330

60. Yip W, Ong PG, Teo BW, et al. Retinal Vascular Imaging Markers and Incident Chronic Kidney Disease: A Prospective Cohort Study. *Sci Rep*. 2017;7:9374. doi:10.1038/s41598-017-09204-2

61. Dumitrescu AG, Voinea L, Badarau IA, Paun VA, Schowe M, Ciuluvica R. Update on retinal vascular caliber. *Rom J Ophthalmol*. 2017;61(3):171-180. doi:10.22336/rjo.2017.32

62. Kannenkeril D, Frost S, Nolde JM, et al. Microvascular changes at different stages of chronic kidney disease. *J Clin Hypertens (Greenwich)*. 2020;23(2):309-316. doi:10.1111/jch.14138

63. Lee SJV, Goh YQ, Rojas-Carabali W, et al. Association between retinal vessels caliber and systemic health: A comprehensive review. *Survey of Ophthalmology*. 2025;70(2):184-199. doi:10.1016/j.survophthal.2024.11.009

64. Liew G, Wang JJ. Retinal vascular signs in diabetes and hypertension--review. *Arq Bras Endocrinol Metabol*. 2007;51(2):352-362. doi:10.1590/s0004-27302007000200027

65. Gao Y, Xu L, He N, et al. A narrative review of retinal vascular parameters and the applications (Part I): Measuring methods. *Brain Circulation*. 2023;9(3):121. doi:10.4103/bc.bc_8_23

66. Gao Y, Xu L, He N, et al. A narrative review of retinal vascular parameters and the applications (Part II): Diagnosis in stroke. *Brain Circ*. 2023;9(3):129-134. doi:10.4103/bc.bc_9_23

67. Barrot J, Real J, Vlacho B, et al. Diabetic retinopathy as a predictor of cardiovascular morbidity and mortality in subjects with type 2 diabetes. *Front Med (Lausanne)*. 2022;9:945245. doi:10.3389/fmed.2022.945245

68. Mordi IR, Trucco E, Syed MG, et al. Prediction of Major Adverse Cardiovascular Events From Retinal, Clinical, and Genomic Data in Individuals With Type 2 Diabetes: A Population Cohort Study. *Diabetes Care*. 2022;45(3):710-716. doi:10.2337/dc21-1124

69. Wong ND, Sattar N. Cardiovascular risk in diabetes mellitus: epidemiology, assessment and prevention. *Nat Rev Cardiol*. 2023;20(10):685-695. doi:10.1038/s41569-023-00877-z